

“THE LONGITUDINAL POLAR CUSP DISPLACEMENT FROM GEOMAGNETIC MEASUREMENTS IN ANTARCTICA”

Martina Marzocchetti¹, Stefania Lepidi^{*,1}, Patrizia Francia², Lili Cafarella¹, Domenico Di Mauro¹

(¹) Istituto Nazionale di Geofisica e Vulcanologia, Roma, Italy

(²) Università degli Studi dell'Aquila, L'Aquila, Italy

Article history

Received October 23, 2018; accepted January 2, 2019.

Subject classification:

Magnetospheric physics; Structure and dynamics; Geomagnetic field variations and reversal; Solar-terrestrial interaction; Space weather

ABSTRACT

We used ULF geomagnetic field measurements in the Pc5 frequency range (1.7–7 mHz) at two Antarctic stations to statistically investigate the longitudinal location of the polar cusp. The two stations are located at the same geomagnetic latitude, ~80° S (just poleward of the cusp), and are separated by one hour in magnetic local time. Since at each station the Pc5 power maximizes when the station approaches the cusp, the comparison between their Pc5 power allows to estimate the longitudinal position of the cusp and to examine its movements. We found that there is a displacement of the cusp depending on interplanetary conditions; in particular, the cusp shifts to later hours for negative values of the interplanetary magnetic field and solar wind velocity east–west components (B_y and V_y), while moves to earlier hours for positive values of V_y . Conversely, no dependence of the cusp longitudinal position on positive B_y values nor on the interplanetary magnetic field north–south component (B_z) emerges.

1. INTRODUCTION

The cusp position is determined in most studies using satellite data [Newell et al. 1989; Stasiewicz 1991; Zhou et al. 1999, 2000; Pitout et al. 2006], in other studies using auroral activity observations [Moen et al. 1999; Bobra et al., 2004; Frey 2007; McEwen et al. 2016]. Also, the ULF Pc5 (1.7 – 7 mHz) power at high geomagnetic latitudes can be indicative of the polar cusp position. Indeed, in a study conducted at stations in a wide

latitudinal interval in the northern hemisphere, Lepidi and Francia [2002] found that in the noon sector the Pc5 power reaches a maximum at ~75° geomagnetic latitude; in addition, it shifts from latitudes slightly lower than 75° during local winter (Nov-Dec-Jan-Feb) and for negative values of the north-south component of the Interplanetary Magnetic Field (IMF, $B_z < 0$) to latitudes of 81–82° during summer and for northward IMF conditions ($B_z > 0$). These findings are consistent with the dependence of the cusp position on season and IMF

conditions obtained by several authors from satellite and optical observations. For example, Zhou et al. [1999] related the observed seasonal dependence with the dipole tilt angle variations, in that when the dipole tilts more toward the Sun, the cusp moves poleward. On the other hand, the IMF B_z and B_y components were found to control the latitude and longitude of the cusp, respectively, with the center of the cusp moving in average from $\sim 80^\circ$ for positive B_z to $\sim 70^\circ$ for strong negative B_z and toward prenoon (postnoon) sector in the northern (southern) hemisphere for negative B_y , and viceversa for B_y positive; moreover, statistically the Magnetic Local Time (MLT) of the footprints of the cusp magnetic field lines was found to extend from 0800 to 1600 MLT with a mean value of 11.7 MLT [Zhou et al., 2000; Frey et al., 2002]. A quantitative estimate of the longitudinal shift of the cusp due to an IMF B_y component, linearly superposed with the magnetospheric field, was given by Stasiewicz [1991] who found that the MLT of the cusp can move by a maximum of 0.07–0.15 hr/nT. More recently, the average local time change of the cusp aurora location for both southward and northward IMF conditions was found to be 0.120–0.127 hr/nT of B_y [Frey et al., 2002; 2003]; it is remarkable, however, that, in the northern hemisphere, Bobra et al. [2004] observed a prenoon location for negative B_y but a large spread in MLT for positive B_y , suggesting further investigations [see the review by Frey, 2007].

In this study the cusp position was estimated from ground-based geomagnetic field data covering the years 2008–2016; in particular, we used the Pc5 power at two Antarctic stations, Mario Zucchelli Station (TNB) and Scott Base (SBA), located at the same Corrected Geo-Magnetic (CGM, <https://omniweb.gsfc.nasa.gov/vitmo/cgm.html>) latitude but separated by 1 hr in MLT (Table 1 and Figure 1), to examine the longitudinal shift of the cusp for different Solar Wind (SW) and IMF conditions. In a previous, recent, study we conducted a similar analysis using TNB and SBA data from one year only, 2002; in that case we found that the cusp longitudinal position was depending on the IMF B_y component, shifting to earlier times for positive B_y [Lepidi et al. 2018]. The wider data set we use in the present study allows to better investigate and quantify the dependence on B_y and, in addition, the dependence on SW flow direction.

2. DATA

We have used 1-min geomagnetic recordings from two fluxgate magnetometers installed at two Antarctic stations, the New Zealand Scott Base Station (SBA),

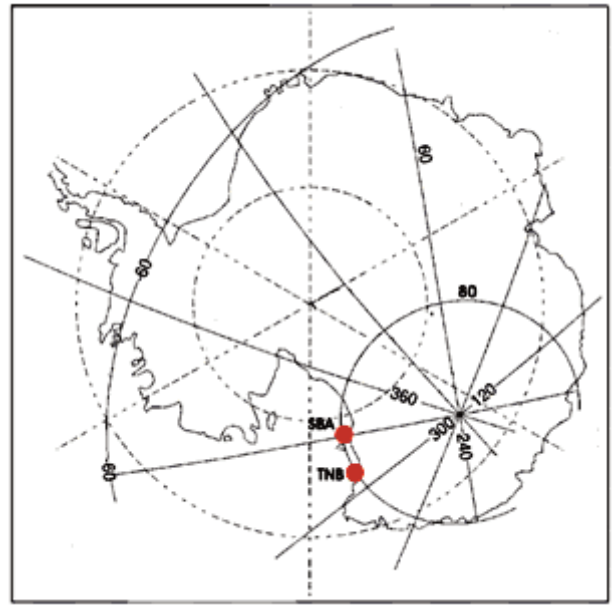


FIGURE 1. Position of TNB and SBA. Dashed and solid lines indicate the geographic and corrected geomagnetic (CGM) coordinate systems, respectively.

Station	Geog. Lat	Geog. Lon	CGM Lat	CGM Lon	MLT noon
TNB	74.7° S	164.1° E	79.9° S	306.7° E	20:16 UT
SBA	77.8° S	166.8° E	79.8° S	326.0° E	19:06 UT

TABLE 1. Geographic and IGRF Corrected Geo–Magnetic coordinates and time in UT of the magnetic local noon for the stations: Mario Zucchelli Station (TNB) and Scott Base (SBA).

whose data are available from the Intermagnet site (<http://www.intermagnet.org>), and the Italian Mario Zucchelli Station located at Terra Nova Bay (TNB). The two stations are separated by 1 hour in MLT, being located at the same Corrected-Geomagnetic Latitude (Table 1 and Figure 1). For the purpose of our study, we have computed the Power Spectral Density (PSD) of the 1-min horizontal component (H) of the geomagnetic field measured at the two stations. Data were differenced (subtracting from each measured value the previous one) before computing the power spectra in order to reduce lower frequency variations. We have computed the PSD over 1 hour overlapping intervals, with 20 minutes shift between consecutive intervals. We have also used the B_x , B_y , B_z components of the IMF in the Geocentric Solar Magnetospheric (GSM) reference system and the V_x and V_y components of the SW in the Geocentric Solar Ecliptic (GSE) reference system (1-min OMNI data, <https://cdaweb.sci.gsfc.nasa.gov/in>

dex.html/). In order to compare these data with the geo-magnetic ones, we have computed the running average of each component over 1 hour intervals with 20 minutes shift between consecutive intervals.

3. EXPERIMENTAL RESULTS

Figure 2 shows the UT-frequency dependence of the average PSD at the two stations. We can see that there is an evident enhancement of the power around local magnetic noon (blue lines indicate the MLT noon from IGRF model) at both stations, independently on frequency. For that reason, we integrated the power over the Pc5 frequency band (1.7-7 mHz); the average Pc5 power very clearly shows the peak around MLT noon at both SBA and TNB (Figure 3). The increase (and decrease) of the power is due to the approaching to (and moving away from) the cusp of both stations, which are anyway located within the polar cap; the maximum power is observed when the stations are at the minimum distance from the cusp, around their MLT noon [Francia et al. 2005]. On the basis of the Pc5 power peak we can deduce the cusp longitudinal position with some approximation, since the power peak is quite broad, covering a few hours around MLT noon at each station; so, in order to define it with more accuracy we have computed the ratio R as the average of the ratios between the Pc5 power at TNB and SBA for each time interval. Moreover, in order to eliminate any systematic difference in power level, due to possible different instrument calibration at the two stations, we subtracted from R its average value computed over the whole time interval. We expect R to be less than one before MLT noon at SBA, greater than one after MLT noon at TNB and equal to one at a time T_0 when the two stations are at the same distance from the cusp. In Figure 4 we show the logarithm of R in the time interval 15-24 UT. This parameter is zero (i.e. logarithm of one) at the time $T_0 \approx 19:35$ UT. Since R = 1 when the cusp is located at a longitude midway between the two stations, we can consider T_0 as indicating the average longitudinal position of the cusp.

We have investigated the T_0 dependence on different SW and IMF parameters. In order to eliminate a possible effect on the cusp longitude of a non-radial SW flow, we evaluated the T_0 dependence on the IMF orientation restricting only to periods with radial SW flow.

We defined the angle

$$\Phi_v = \tan^{-1}(V_y/V_x)$$

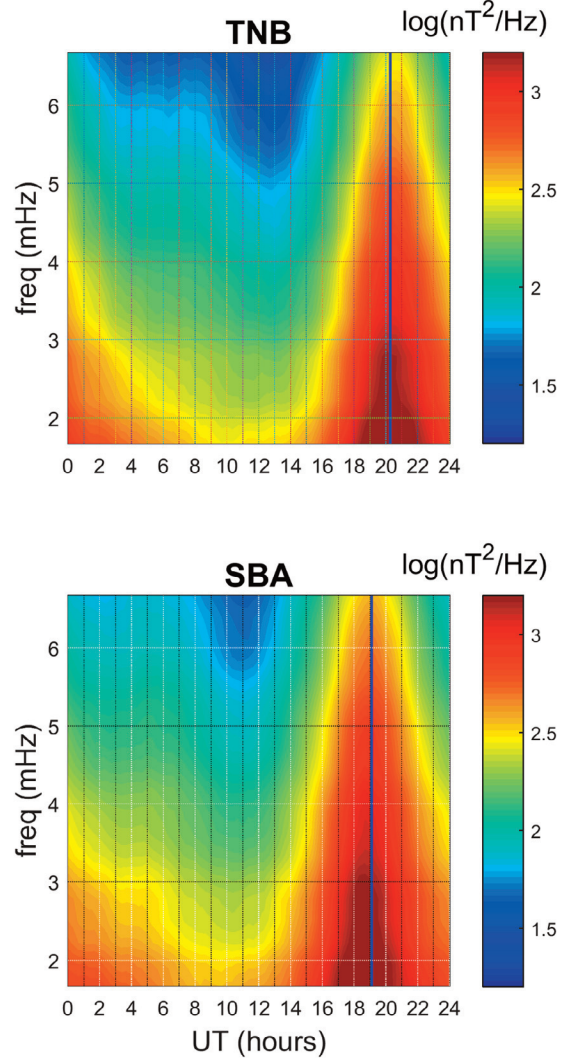


FIGURE 2. The UT dependence of the average power spectra in the Pc5 frequency range. Blue vertical lines indicate the MLT noon from IGRF model.

which is positive (negative) for SW flow directed westward (eastward). Figure 5a shows the Φ_v values distribution. We used Φ_v as sorting parameter for radial SW velocity, which corresponds to Φ_v values close to zero (we chose $-3^\circ \leq \Phi_v \leq 3^\circ$ to have a good statistic).

We investigated the dependence of T_0 on the IMF orientation, using the IMF clock angle

$$\theta = \tan^{-1}(B_y/B_z)$$

whose distribution is shown in Figure 5b, along with those of B_y and B_z (Fig. 5c and 5d). Figure 6 shows the logarithm of R in function of UT for 8 different sectors, corresponding to different IMF orientation in the y-z plane (each sector is represented by the black area in the polar diagram inserted in each plot). We can see that in

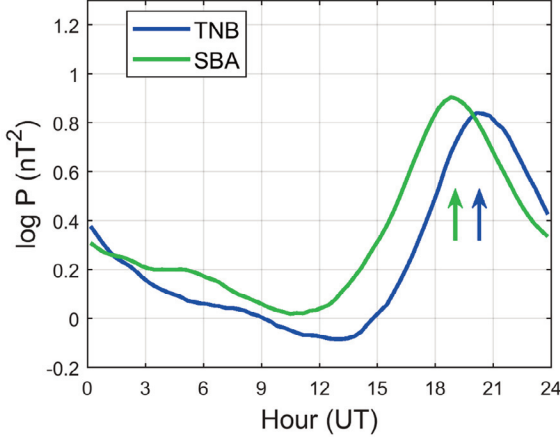


FIGURE 3. The Pc5 integrated power for the two stations (TNB blue line and SBA green line). The two arrows indicate the MLT noon from IGRF model for TNB (blue) and SBA (green).

the sectors corresponding to negative B_z ($-180^\circ \leq \theta \leq -90^\circ$ and $90^\circ \leq \theta \leq 180^\circ$), especially when B_z is dominant ($-180^\circ \leq \theta \leq -135^\circ$ and $135^\circ \leq \theta \leq 180^\circ$), R increases more slowly from minimum to maximum values ($\sim 5\text{-}6$ hours) with respect to positive B_z sectors ($\sim 2\text{-}3$ hours), indicating a wider longitudinal width of the cusp.

For the different θ sectors we estimated the T_0 values, whose dependence on θ is shown in Figure 7. It can be seen that T_0 is quite stable, around 19:20–19:30 UT, except for the two sectors corresponding to both negative B_z and B_y (i.e. $-180^\circ \leq \theta < -135^\circ$ and $-135^\circ \leq \theta < -90^\circ$); in particular, it reaches almost 20 UT for dominant, negative B_y ($-135^\circ \leq \theta < -90^\circ$).

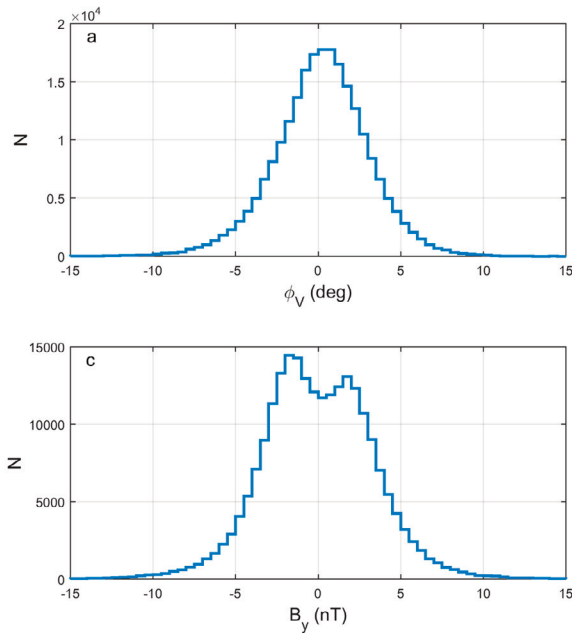


FIGURE 5. Φ_V (panel a), θ (panel b), B_y (panel c) and B_z (panel d) distribution from 2008 to 2016.

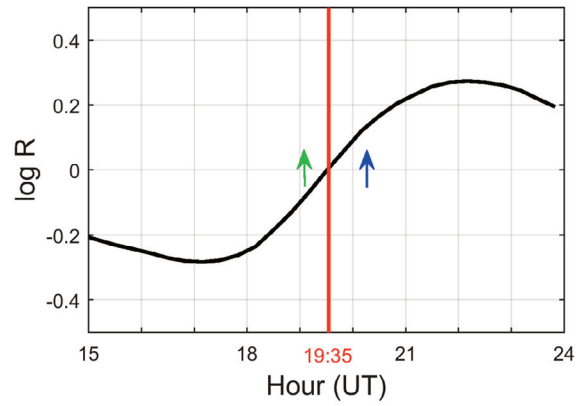
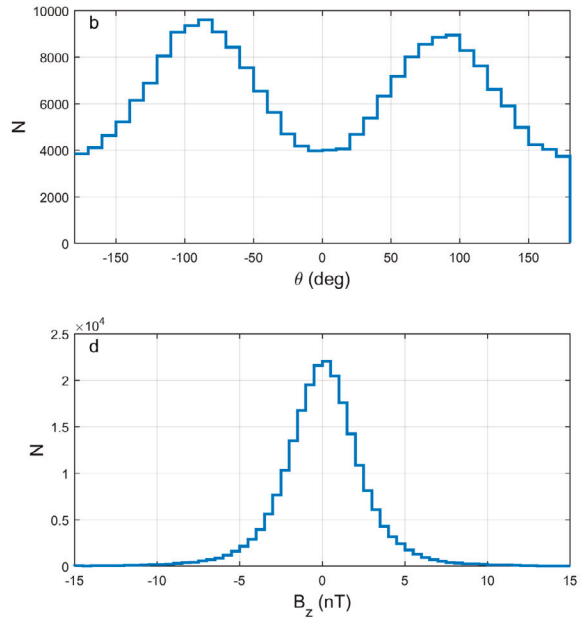


FIGURE 4. The logarithmic average ratio R between the Pc5 power at TNB and SBA from 15 UT to 24 UT, i.e. around MLT noon. The red line indicates $T_0 \approx 19:35$ UT. The two arrows indicate the MLT noon from IGRF model for TNB (blue) and SBA (green).

We then investigated the dependence of T_0 on B_y ; we determined the T_0 value for different B_y intervals with 2 nT amplitude between -4 nT and 4 nT, and for the two extreme intervals $B_y < -4$ nT and $B_y > 4$ nT, separately for positive and negative B_z (Figure 8, red and blue lines, respectively). We see that T_0 is stable (around 19:25–19:30 UT) for positive B_y . Conversely, for negative B_y it shifts to later times for increasing B_y absolute values; the observed shift is greater for negative B_z conditions, reaching 20:30 UT for $B_y < -4$ nT. The MLT change of the cusp location can be estimated to be about 0.1 hr/nT for $B_z > 0$ and 0.25 hr/nT for $B_z < 0$.



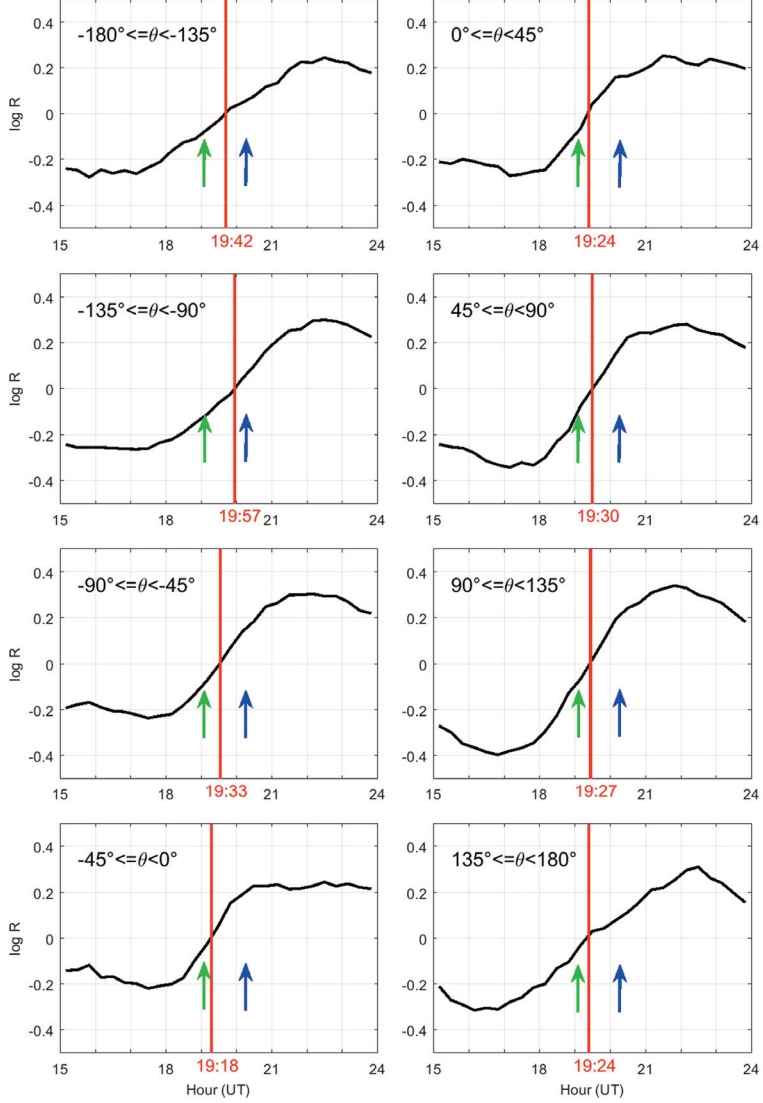


FIGURE 6. The logarithmic average ratio R for radial SW flow and for 8 different θ sectors, corresponding to different IMF orientation in the y - z plane (each sector is represented by the black area in the polar diagram inserted in each plot). The red lines indicate T_0 and the arrows indicate MLT noon from IGRF model for TNB (blue) and SBA (green).

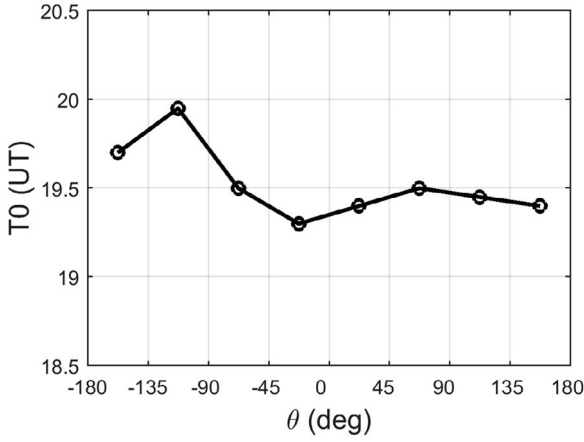


FIGURE 7. T_0 dependence on θ for radial SW flow. Each point corresponds to a θ sector of Fig. 6.

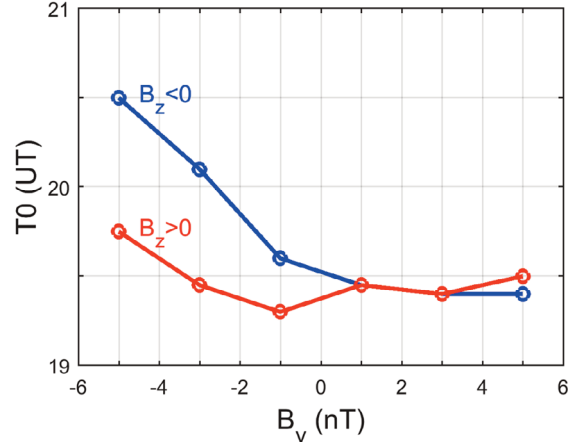


FIGURE 8. T_0 dependence on B_y for radial SW flow: the blue line shows the cases when B_z is negative, while the red line when B_z is positive.

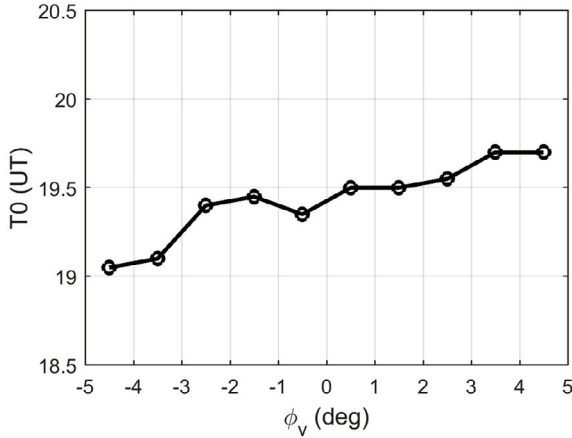


FIGURE 9. T_0 dependence on Φ_V for positive B_y .

We lastly investigated the T_0 dependence on θ_V ; for this purpose we considered only intervals with positive B_y to remove the IMF orientation dependence observed in Fig. 8. We determined the T_0 value for different θ_V intervals with 1° amplitude between -4° and 4° , and for the two extreme intervals $\theta_V < -4^\circ$ and $\theta_V > 4^\circ$. The results in Fig. 9 show a systematic increase of T_0 for increasing θ_V , from $T_0 \approx 19:05$ for $\theta_V < -4^\circ$ (eastward SW flow) to $T_0 \approx 19:40$ for $\theta_V > 4^\circ$ (westward SW flow), indicating that the cusp longitudinal position changes in response to the SW flow direction. Consistently with previous results for positive B_y and radial SW flow, we can observe $T_0 \sim 19:25$ UT when $\theta_V \sim 0$.

4. CONCLUSIONS

In this paper we analyzed the dependence of the longitudinal position of the southern polar cusp on SW and IMF parameters. Most previous studies on polar cusp position are based on satellite data [Newell et al. 1989; Stasiewicz 1991; Zhou et al. 1999, 2000; Pitout et al. 2006] or on auroral activity observations [Moen et al. 1999; McEwen et al. 2016], while in our study the longitudinal position of the cusp was determined using geomagnetic ground based data. The advantage of our alternative method is the availability of long, continuous series of geomagnetic data which cover, with good statistics, different magnetospheric conditions. In particular, using data between 2008 and 2016, we computed the average ratio between the integrated Pc5 power at two longitudinally spaced Antarctic stations at the same CGM latitude (-80°S); the time dependence of the logarithm of this ratio shows a bipolar behavior, because the two stations reach minimum distance from the polar cusp in consecutive times, passing through zero at a time when the

cusp longitude is located midway between the two stations. This time, representing the average longitudinal position of the cusp, is 19:35 UT; it is slightly in advance with respect to the time in the middle between the local geomagnetic noon at TNB and SBA (20:16 UT and 19:06 UT, respectively); consistently, also Frey et al. [2002] found that the average cusp position in local time is earlier (11.7 MLT) than the MLT noon. The analysis conducted for different SW and IMF conditions allows to estimate the longitudinal movements of the cusp.

We found that the longitudinal position of the dayside cusp depends on:

- 1) the azimuthal component of the IMF, shifting to later times for increasing negative B_y (while positive B_y seems to have no effect). The observed shift for positive B_z is small (about 0.1 hr/nT) and consistent with previous estimates [Stasiewicz, 1991; Frey et al., 2002; 2003] while, unlike these, it tends to be much greater for $B_z < 0$ (about 0.25 hr/nT).
- 2) the azimuthal component of the SW flow: the cusp position shifts of ≈ 40 minutes for deviation of about 10° of SW velocity direction with respect to the Sun-Earth direction, consistently with the shift of the point where the SW flow impacts perpendicularly on the magnetopause, i.e. toward earlier (later) times for eastward (westward) SW flow.

The position of the cusp, when the influence of B_y and of the SW flow direction is negligible (i.e. for positive B_y and radial SW), is at $\sim 19:25$ - $19:30$ UT, in advance with respect to its average value of 19:35 UT and then further in advance to the time in the middle between the MLT noon at the two stations.

We also found that the B_z component, which is known to influence the cusp latitudinal position [Newell et al. 1989; Stasiewicz 1991; Zhou et al. 2000; Lepidi and Francia, 2002; Pitout et al. 2006], does not seem to have the predominant role in determining the cusp longitudinal position. Conversely, our results suggest that B_z influences the longitudinal width of the cusp, which is wider for negative B_z ; our results are then consistent with the MLT extent of the cusp found by Newell et al. [2007], i.e. an increase from 2.33 hours for low merging rate to 3.45 hours for high merging rate.

The use of ground-based data is then a powerful tool, especially for statistical studies, and a reliable alternative to satellite data. Making a coordinated study also with cusp observations by other means, i.e. spacecraft or auroral imagers, when simultaneous observations are available, would obviously strengthen the validity of our technique.

5. DATA AND SHARING RESOURCES

TNB data can be downloaded from the INGV web site: <http://geomag.rm.ingv.it/index.php>. SBA data can be downloaded from the INTERMAGNET web site: <http://www.intermagnet.org>. Solar Wind and Interplanetary Magnetic Field data can be downloaded from: <https://cdaweb.sci.gsfc.nasa.gov/index.html/>

Acknowledgements. The research activity at Mario Zucchelli station has been supported by the Italian PNRA (Programma Nazionale Ricerche in Antartide). The results presented in this paper rely on the data collected at Scott Base; we thank the Institute of Geological & Nuclear Sciences Limited (New Zealand), for supporting its operation and INTERMAGNET for promoting high standards of magnetic observatory practice (<http://www.intermagnet.org>).

REFERENCES

- Bobra, M. G., S. M. Petrinec, S. A. Fuselier, E. S. Claflin, and H. E. Spence (2004). On the solar wind control of cusp aurora during northward IMF, *Geophys. Res. Lett.*, 31, L04805, doi:10.1029/2003GL018417.
- Francia, P., L.J. Lanzerotti, U. Villante, S. Lepidi and D. Di Memmo (2005). A statistical analysis of low-frequency magnetic pulsations at cusp and cap latitudes in Antarctica, *J. Geophys. Res.*, 110, A02205, doi: 10.1029/2004JA010680.
- Frey, H. U., S. B. Mende, T. J. Immel, S. A. Fuselier, E. S. Claflin, J.-C. Gérard, and B. Hubert (2002). Proton aurora in the cusp, *J. Geophys. Res.*, 107(A7), 1091, doi:10.1029/2001JA900161.
- Frey, H. U., S. B. Mende, S. A. Fuselier, T. J. Immel, and N. Østgaard (2003). Proton aurora in the cusp during southward IMF, *J. Geophys. Res.*, 108(A7), 1277, doi:10.1029/2003JA009861.
- Frey, H. U. (2007). Localized aurora beyond the auroral oval, *Rev. Geophys.*, 45, RG1003, doi:10.1029/2005RG000174.
- Lepidi, S. and P. Francia (2002). Low frequency (~1–4 mHz) geomagnetic field fluctuation power: longitudinal dependence and relation with solar wind parameters, *Proceedings SOLSPA: The Second Solar Cycle and Space Weather Euroconference*, Vico Equense (Italy), Sept. 24–29, 2001, ESA SP-477, 447–450.
- Lepidi, S., P. Francia, L. Cafarella, D. Di Mauro and M. Marzocchetti (2018). Determining The Polar Cusp Longitudinal Location From Pc5 Geomagnetic Field Measurements At A Pair Of High Latitude Stations, in press in: *Space Weather of the Heliosphere: Processes and Forecasts, Proceedings IAU Symposium*, A.C. Editor, B.D. Editor & C.E. Editor, No. 335.
- McEwen, D.J., G.G. Sivjee and Y. Zhang (2016). Dynamics of the dayside aurora as viewed from the South Pole, *Auroral Dynamics and Space Weather*, 1, *Geophysical Mon.* 215, Y. Zhang and L.J. Paxton (Editors), AGU.
- Moen, J., H.C. Carlson and P.E. Sandholt (1999). Continuous observation of cusp auroral dynamics in response to an IMF By polarity change, *Geophys. Res. Lett.*, 26, 12431246.
- Newell, P.T., C.I. Meng, D. Sibeck and R. Lepping (1989). Some low altitude cusp dependencies on the interplanetary magnetic field, *J. Geophys. Res.*, 94, 89218927.
- Newell, P. T., S. Wing, and F. J. Rich (2007), Cusp for high and low merging rates, *J. Geophys. Res.*, 112, A09205, doi:10.1029/2007JA012353.
- Pitout, F., C.P. Escoubet, B. Klecker and H. Reme (2006). Cluster survey of the mid-altitude cusp: 1. Size, location, and dynamics, *Ann. Geophysicae*, 24, 30113026.
- Staisiewicz, K. (1991). Polar cusp topology and position as a function of interplanetary magnetic field and magnetic activity: comparison of a model with Viking and other observations, *J. Geophys. Res.*, 96, doi: 10.1029/91JA01420.
- Zhou, X.W., C.T. Russel, G. Le., S.A. Fuselier and J.D. Scudder (1999). The polar cusp locations and its dependence on dipole tilt, *Geophys. Res. Lett.*, 26, 429432.
- Zhou, X.W., C.T. Russel, G. Le., S.A. Fuselier and J.D. Scudder (2000). Solar wind control of the polar cusp at high altitude, *J. Geophys. Res.*, 105, 245252.

*CORRESPONDING AUTHOR: Stefania LEPIDI,

Istituto Nazionale di Geofisica e Vulcanologia,

L'Aquila, Italy

email: stefania.lepidi@ingv.it

© 2019 the Istituto Nazionale di Geofisica e Vulcanologia.

All rights reserved